ISSN No: 2348-4845
International Journal & Magazine of Engineering, Technology, Management and Research
A Peer Reviewed Open Access International Journal

Power Quality Improvement in Load Transformers by Using Series Voltage Sag Compensator

P.SUDHEER*, B.HARI PRASAD, G.N.S.VAIBHAV***,**
*(PG student, Department of Electrical & Electronics Engineering, P.V.K.K Institute of Technology)
** (Assistant Professor, Department of Electrical & Electronics Engineering, P.V.K.K Institute of Technology)
*** (Head of the Department of Electrical & Electronics Engineering, P.V.K.K Institute of Technology)

Abstract— The proposed paper, Survey results recommend that 92% of intrusion at mechanical offices is voltage hang related. The voltage list compensator, in light of a transformer-coupled arrangement associated voltage-source inverter, is among the most savvy arrangement against voltage hangs. At the point when voltage lists happen, the transformers, which are frequently introduced before discriminating burdens for electrical disengagement, are presented to the deformed voltages and a dc counterbalance will happen in its flux linkage. At the point when the compensator restores the heap voltage, the flux linkage will be determined to the level of attractive immersion and serious inrush current happens. The compensator is liable to be intruded on as a result of its own over present insurance, and in the long run, the remuneration fizzles, and the basic burdens are hindered by the voltage droop. This paper proposes an inrush current relief system together with a state-input controller for the voltage droop compensator. The operation standards of the proposed system are particularly exhibited, and tests are given to accept the proposed methodology.

Keywords: Flux linkage, inrush current, power quality, transformer, voltage sag, voltage sag compensator.

I. INTRODUCTION

POWER quality issues have gotten much consideration as of late. In numerous nations, innovative producers move in industry parks. Accordingly, any force quality occasions in the utility network can influence countless. Records demonstrate that voltage list, homeless people, and passing interference constitute 92% of the force quality issues [1]. Voltage droops regularly interfere with discriminating loads and results in significant profit misfortunes. Commercial ventures have embraced the voltage hang compensators as a standout amongst the most financially savvy ride-through arrangements [2]–[7], and most compensators can finish voltage rebuilding inside a quarter cycle. Then again, the heap transformer is uncovered under the disfigured voltages before the reclamation, and attractive flux deviation may be produced inside the heap transformers. When the heap voltage is restored, the attractive flux may further float past the immersion knee of the center and lead to huge inrush current. The over present insurance of the compensator could be effectively activated and lead to recompense disappointment.

Different transformer inrush diminishment procedures have been exhibited, such as controlling force on point and the voltage size [8]–[12], or effectively controlling the transformer mongrel rent [13]–[15]. These systems could undoubtedly change the yield voltage waveforms of the converter, and therefore, is not suitable for voltage list compensator, which request exact point-on-wave reclamation of the heap voltages.

In this paper, the inrush issue of burden transformers under the operation of the list compensator is introduced. An inrush alleviation procedure is proposed and actualized in a synchronous reference outline voltage hang compensator controller. The proposed system can be incorporated with the traditional shut circle control on the heap voltages. The new incorporated control can effectively lessen inrush present of burden trans-formers and enhance the aggravation dismissal capacity and the heartiness of the hang compensator framework. Research facility test outcomes are introduced to approve the proposed framework.

II. SYSTEM CONFIGURATION OF THE PROPOSED COMPENSATOR

As shown in Fig. 1, the voltage sag compensator consists of a three-phase voltage-source inverter (VSI) and a coupling

ISSN No: 2348-4845
International Journal & Magazine of Engineering, Technology, Management and Research
A Peer Reviewed Open Access International Journal

transformer for serial connection. When the grid is normal, the compensator is bypassed by the thyristors for high operating efficiency. When voltage sags occur, the voltage sag compensator injects the required compensation voltage through the coupling transformer to protect critical loads from being interrupted. However, certain detection time (typically within 4.0 ms) is required by the sag compensator controller to identify the sag event [16]–[18]. And the load transformer is exposed to the de-formed voltage from the sag occurrence to the moment when the compensator restores the load voltage. Albeit its short duration, the deformed voltage causes magnetic flux deviation inside the load transformer, and the magnetic saturation may easily occur when the compensator restores the load voltage, and thus, results in the inrush current. The inrush current could trigger the over current protection of the compensator and lead to compensation failure. Thus, this paper proposes an inrush mitigation technique by correcting the flux linkage offsets of the load transformer, and this technique can be seamlessly integrated with the state-feedback controller of the compensator.

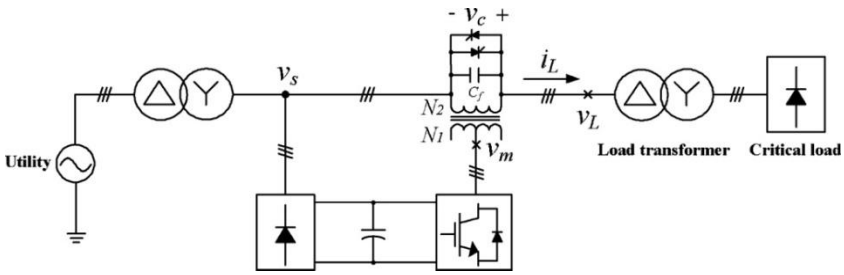

Fig. 1. Simplified one-line diagram of the offline series voltage sag compensator.

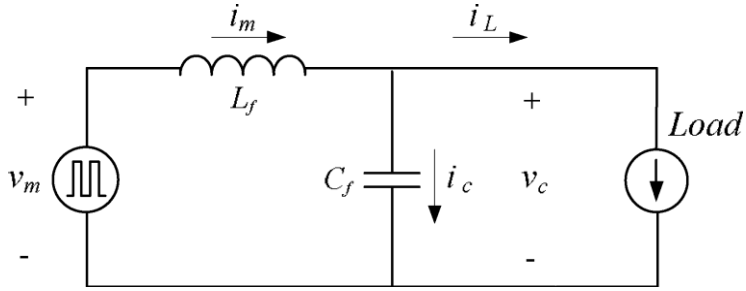

Fig.2. Per-phase equivalent circuit of the series voltage sag compensator.

The dynamics of the sag compensator will be described. The proposed inrush mitigation technique and its integration with the voltage and current closed-loop controls are also presented.

A. Dynamics of the Sag Compensator

The dynamics of the sag compensator can be represented by an equivalent circuit in Fig. 2. Generally, the sag compensator is rated for compensating all three-phase voltages down to 50% of nominal grid voltage. The coupling transformer is capable of electrical isolation or boosting the compensation voltage. In the proposed system, the turns ratio of the coupling transformer is set on unitary (N1:N2 = 1:1) to provide the maximum compensation voltage of the 50% of nominal value. Moreover, the leakage inductor of the coupling transformer is used as the filter inductor Lf and is combined with the filter capacitor C_f installed in the secondary winding of the coupling transformer to suppress pulse width modulated (PWM) ripples of the inverter output voltage v_m. The dynamics equations are expressed as follows:

$$L_f \frac{d}{dt}\begin{bmatrix} i_{ma} \\ i_{mb} \\ i_{mc} \end{bmatrix} = \begin{bmatrix} v_{ma} \\ v_{mb} \\ v_{mc} \end{bmatrix} - \begin{bmatrix} v_{ca} \\ v_{cb} \\ v_{cc} \end{bmatrix} \quad (1)$$

$$C_f \frac{d}{dt}\begin{bmatrix} v_{ca} \\ v_{cb} \\ v_{cc} \end{bmatrix} = \begin{bmatrix} i_{ma} \\ i_{mb} \\ i_{mc} \end{bmatrix} - \begin{bmatrix} i_{La} \\ i_{Lb} \\ i_{Lc} \end{bmatrix} \quad (2)$$

ISSN No: 2348-4845
International Journal & Magazine of Engineering, Technology, Management and Research
A Peer Reviewed Open Access International Journal

Where $[v_{ma}\ v_{mb}\ v_{mc}]\ T$ is the inverter output voltage, $[i_{ma}\ i_{mb}\ i_{mc}]\ T$ is the filter inductor current, $[v_{ca}\ v_{cb}\ v_{cc}\ ]\ T$ is the compensation voltage, and $[i_{La}\ i_{Lb}\ i_{Lc}]T$ is the load current. Equations (1) and (2) are transformed into the synchronous reference frame as the following:

$$\frac{d}{dt}\begin{bmatrix} i^e_{mq} \\ i^e_{md} \end{bmatrix} = \begin{bmatrix} 0 & -\omega \\ \omega & 0 \end{bmatrix}\begin{bmatrix} i^e_{mq} \\ i^e_{md} \end{bmatrix} + \frac{1}{L_f}\begin{bmatrix} v^e_{mq} \\ v^e_{md} \end{bmatrix} - \frac{1}{L_f}\begin{bmatrix} v^e_{cq} \\ v^e_{cd} \end{bmatrix} \quad (3)$$

$$\frac{d}{dt}\begin{bmatrix} v^e_{cq} \\ v^e_{cd} \end{bmatrix} = \begin{bmatrix} 0 & -\omega \\ \omega & 0 \end{bmatrix}\begin{bmatrix} v^e_{cq} \\ v^e_{cd} \end{bmatrix} + \frac{1}{C_f}\begin{bmatrix} i^e_{mq} \\ i^e_{md} \end{bmatrix} - \frac{1}{C_f}\begin{bmatrix} i^e_{Lq} \\ i^e_{Ld} \end{bmatrix} \quad (4)$$

Where superscript "e" indicates the synchronous reference frame representation of this variable and ω is the angular frequency of the utility grid. Equations (3) and (4) show the cross-coupling terms between the compensation voltage and the filter inductor current. The block diagram of the physical circuit dynamics are illustrated in the right-hand side of Fig. 3. B. Voltage and Current Closed-Loop Controls Fig. 3 shows the block diagram of the proposed control method. Note that the d-axis controller is not shown for simplicity. The block diagram consists of the full state-feedback controller [19]–[22] and the proposed inrush current mitigation technique. The feedback control, feed forward control, and decoupling control are explained as follows.

1) Feedback Control: The feedback control is to improve the precision of the compensation voltage, the disturbance rejection capability, and the robustness against parameter variations.
As shown in Fig. 3, the capacitor voltage v^e_{cq} and the inductor current i^e_{mq} are handled by the outer-loop voltage control and the inner-loop current control, respectively. The voltage control is implemented by a proportional gain K_{pv} with a voltage command v^{e*}_{cq} produced by the voltage sag compensation scheme.
The current control also consists of a proportional control gain K_{pi} to accomplish fast current tracking.
2) Feed forward Control: To improve the dynamic response of the voltage sag compensator, the feed forward control is added to the voltage controller to compensate the load voltage immediately when voltage sag occurs. The feed forward voltage command can be calculated by combining the compensation voltage and the voltage drop across the filter inductor L_f.
3) Decoupling Control: The cross-coupling terms are the result of the synchronous reference frame transformation, as in (3) and 4). The controller utilizes the decoupling terms to negate the cross coupling and reduce the interferences between

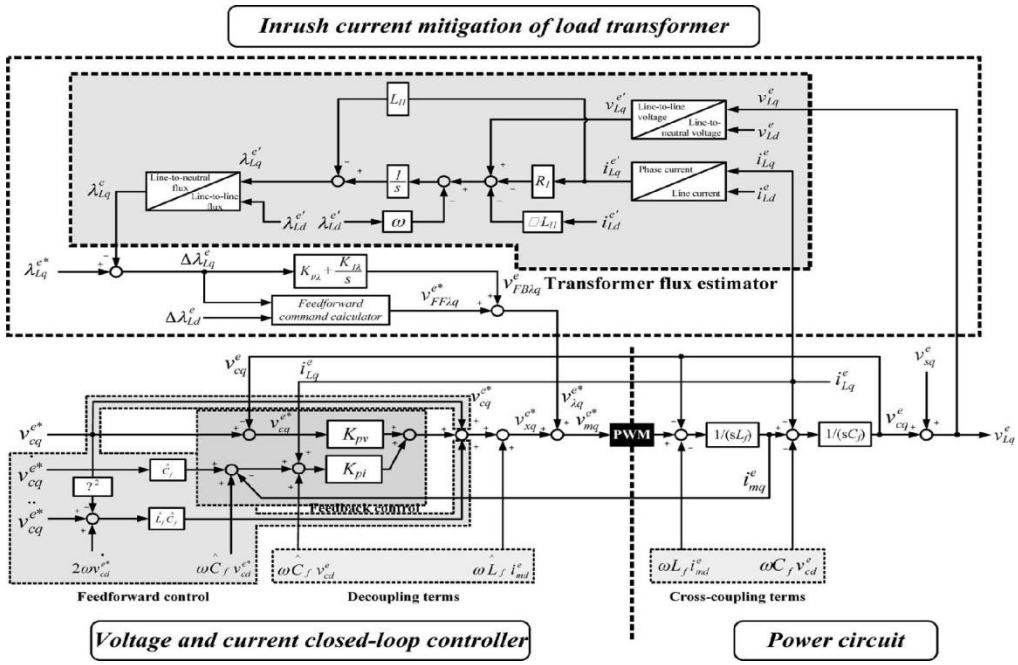

ISSN No: 2348-4845
International Journal & Magazine of Engineering, Technology, Management and Research
A Peer Reviewed Open Access International Journal

Fig. 3. Block diagram of the proposed inrush current mitigation technique with the state-feedback control.

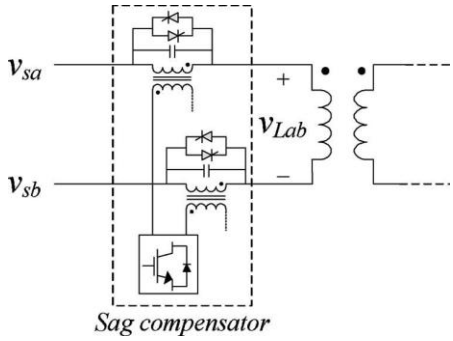

Fig. 4. Connection diagram of the proposed system and the delta/wye load transformer.

the *d–q* axes. Fig. 3 shows that the decoupling terms can be accomplished by the filter capacitor voltage v^{e}_{cd} , the filter inductor current i^{e}_{md} , and the estimated values of the filter capacitor and the filter inductor.

C. Inrush Current Mitigation Technique

1) *Flux Linkage Deviation due to Sags:* Fig. 4 shows the equivalent circuit of the phase *a* and *b* winding of the delta/wye three-phase load transformer installed in downstream of the voltage sag compensator. The flux linkage of the phase *a* and *b* winding is expressed as follows:

$$\lambda_{Lab}(t) = \int^{t} v_{Lab}(\tau)d\tau. \qquad (5)$$

Fig. 5 illustrates the line-to-line voltage across the transformer winding and the resulting flux linkage from the sag occurrence to completion of the voltage compensation.

When voltage sag occurs ($t = t_{sag}$), the controller detects the sagged voltage and injects the required compensation voltage at $t = t_{raction,}$. The flux linkage of the transformer winding *a* and *b* during the voltage compensation process can be expressed as following:

$$\lambda_{Lab}(t) = \lambda_{Lab}(t)|_{t-t_{sag}} + \int_{t_{sag}}^{t_{action}} v_{Lab}(\tau)\,d\tau + \int_{t_{action}}^{t} v^{*}_{Lab}(\tau)\,d\tau \qquad (6)$$

Where v^{*}_{Lab} is the normal load voltage defined as follows:

$$v^{*}_{Lab}(t) = \hat{V}^{*}_{Lab}\sin(\omega t + \Phi^{*}_{Lab}) \qquad \forall t.$$

ISSN No: 2348-4845
International Journal & Magazine of Engineering, Technology, Management and Research
A Peer Reviewed Open Access International Journal

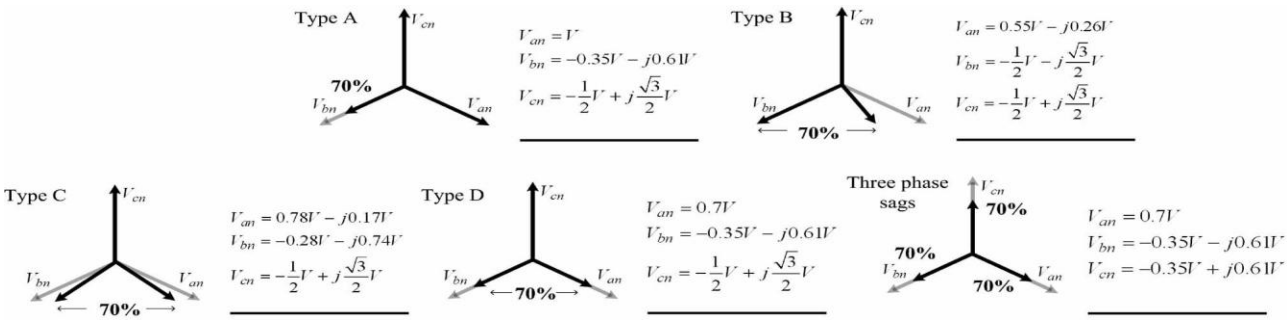

Fig. 6. Phasor diagram of the utility voltage under the various types of voltage sags (V: voltage magnitude of the normal state) [23].

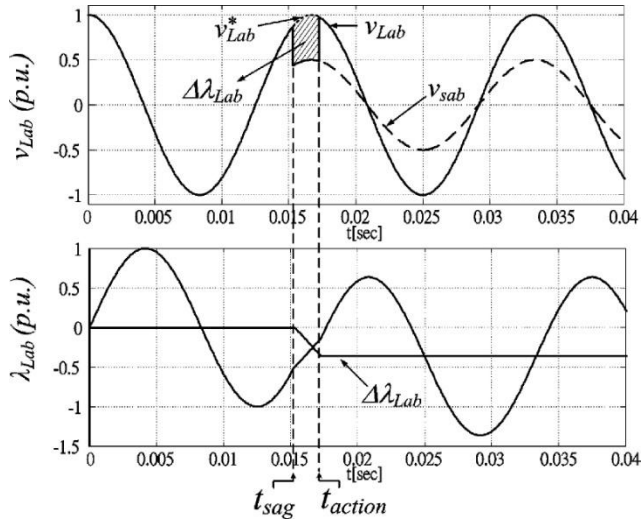

Fig. 5. Transformer voltage and corresponding transient flux linkage.

Equation (6) can be rewritten as follows:

$$v_{Lab}(t) = \hat{V}^{*}_{Lab}(1-u)\sin(\omega t + \Phi^{*}_{Lab} + \theta_{Lab})$$
$$\text{for} \quad t_{sag} \le t \le t_{action}$$

whereV^{*}_{Lab} is the magnitude of load voltage, is the grid frequency, and Φ^{*}_{Lab} is the phase angle. Thus, after the voltage compensation is completed, the flux linkage can be expressed as follows:

ISSN No: 2348-4845
International Journal & Magazine of Engineering, Technology, Management and Research
A Peer Reviewed Open Access International Journal

$$\lambda_{Lab}(t) = \lambda_{Lab}(t)|_{t-t_{sag}} - \int_0^{t_{sag}} v^*_{Lab}(\tau)\, d\tau + \int_{t_{sag}}^{t_{action}} (v_{Lab}(\tau) - v^*_{Lab}(\tau))d\tau + \int_0^t v^*_{Lab}(\tau)\, d\tau \quad (7)$$

where,

$$\lambda_{Lab}(t) = \Delta\lambda_{Lab}(t)|_{t-t_{action}} + \frac{\hat{V}^*_{Lab}}{\omega}\sin\left(\omega t + \Phi^*_{Lab} - \frac{\pi}{2}\right) \quad \text{for} \quad t \geq t_{action} \quad (8)$$

The flux linkages of other transformer windings can also be derived by the same procedures. Equation (9) states that the sagged voltages cause the flux-linkage dc offset $\Delta\lambda_{L\,ab}$ on the transformer windings, and its magnitude is dependent on the depth, the duration, and the point-on-wave of sagged voltages. In the paper, the IEEE P1668 standard is utilized to investigate the flux linkage deviation of the load transformer caused by the line fault, where the phasor diagram of the utility voltage under the various types of voltage sags is given in Fig. 6 [23]. Assuming that the deformed grid voltage imposed upon the load transformer is

$$\Delta\lambda_{Lab}(t)|_{t-t_{action}} = \int_{t_{sag}}^{t_{action}} (v_{Lab}(\tau) - v^*_{Lab}(\tau))\, d\tau. \quad (9)$$

Where u ($0 \leq u \leq 1.0$) is depth of voltage sag and $\theta_{L\,ab}$ is the phase shift during the fault event. According to (9), Fig. 7 shows the analytical results of the maximum flux linkage deviation of all three transformer windings, assuming the load transformer (with delta/wye connection) is exposed to various types of the voltage sags of IEEE P1668 for the range of 1.0–6.0 ms before the voltage is restored by the sag compensator. Along different point-on-wave of voltage sags, the maximum value of flux linkage deviation reaches 36%–62% after the sag compensator is started, as shown in Fig. 7, which could easily induce a significant inrush current. Based on the *B–H* curve of the transformer core, Fig. 7 can be utilized to evaluate the effect of the voltage sags on the transformer flux linkage deviation and the magnitude of resulting inrush current. If the load transformer has a low-saturation threshold, large flux linkage deviation incorporating a high inrush current will pose a great risk for the sag compensator and the critical loads.

2) Design of the Flux Linkage Estimator: Fig. 8 is a per-phase model of a three-phase transformer under load, where R_1 and R_2 represent the copper losses, $L_{l\ 1}$ and $L_{l\ 2}$ are the equivalent leakage inductances, R_c represents the core losses, is the magnetizing inductance.

The dynamics equation of the load transformer can be represented in the synchronous reference frame as follows:

$$s\begin{bmatrix}\lambda^e_{Lq}\\ \lambda^e_{Ld}\end{bmatrix} = \begin{bmatrix}v^e_{Lq}\\ v^e_{Ld}\end{bmatrix} - (R_1 + L_{l1}s)\begin{bmatrix}i^e_{Lq}\\ i^e_{Ld}\end{bmatrix}$$

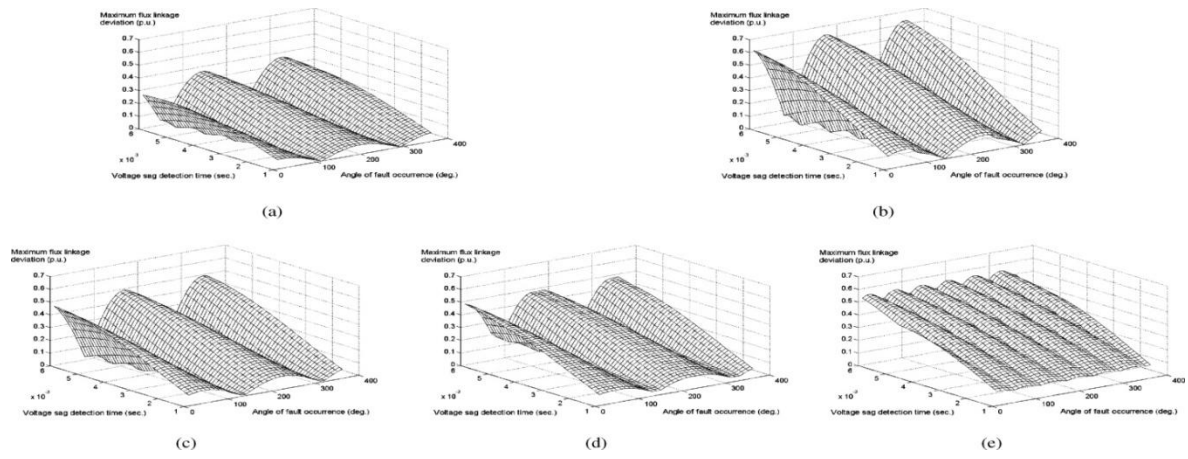

(a) (b) (c) (d) (e)

ISSN No: 2348-4845
International Journal & Magazine of Engineering, Technology, Management and Research
A Peer Reviewed Open Access International Journal

Fig. 7. Maximum flux linkage deviation of the load transformer with the delta/wye connection under the various types of voltage sags (IEEE P1668).
(a) Type A. (b) Type B. (c) Type C. (d) Type D. (e) Three-phase sags.

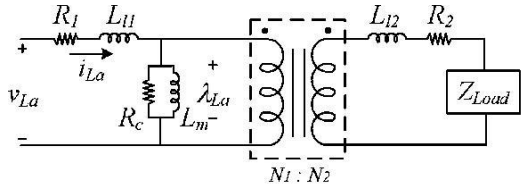

Fig. 8. Equivalent per-phase circuit model of the load transformer.

$$- L_{l1} \begin{bmatrix} 0 & \omega \\ -\omega & 0 \end{bmatrix} \begin{bmatrix} i^e_{Lq} \\ i^e_{Ld} \end{bmatrix} - \begin{bmatrix} 0 & \omega \\ -\omega & 0 \end{bmatrix} \begin{bmatrix} \lambda^e_{Lq} \\ \lambda^e_{Ld} \end{bmatrix} \quad (10)$$

Where the frequency ω (=377 rad/s) is the angular frequency of the utility grid. A flux linkage estimator based on (10) can be implemented, as shown in Fig. 9. This transformer flux estimation scheme is applied to the proposed inrush mitigation technique, which includes the feedback and feed forward control of the flux linkage.

The integration of voltage and current closed-loop controllers and the transformer flux estimator are shown in Fig. 3. In the control block diagram, the flux estimator is used for the load transformer with delta–wye connection. Thus, a transformation from the line-to-neutral voltage to the line-to-line voltage is ap-plied to obtain the voltages across the transformer windings. In practical applications, moreover, the integrator in the proposed flux estimator is usually implemented as the low-pass filter with an extremely low cutoff frequency ($1/(s + \omega_c)$) to provide sta-bility and avoid any accumulative errors caused by the signal offset from the transducers and the analog/digital converters.

In the feedback control loop, the flux linkage command $\lambda^e{}_{L}{}^{*}{}_{q}$ is calculated based on prefault load voltage $v_L{}^e{}_q$, and the estimated flux linkage $\lambda^e{}_{L\,q}$ is generated by the flux linkage estimator in

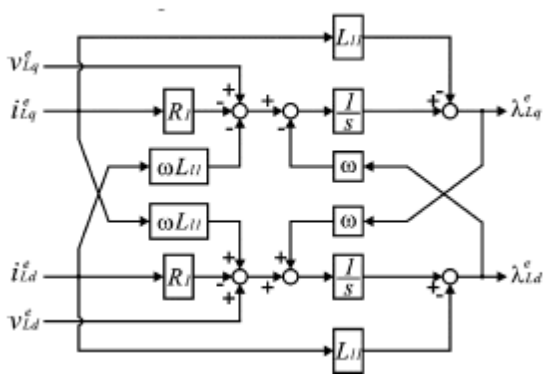

Fig. 9. Proposed flux linkage estimator under the synchronous reference frame.
Fig. 9. The error between $\lambda^e{}_{L}{}^{*}{}_{q}$ and $\lambda^e{}_{L\,q}$ is regulated by a PI regulator.

To speed up the dynamics response of the inrush current mitigation, the estimated flux linkage deviation $\Delta\lambda^e{}_{L\,q}$ $(=\lambda^e{}_{L}{}^{*}{}_{q} - \lambda^e{}_{L\,q})$ is also utilized as a feed forward control term. The feed forward command calculator can generate a suitable feed-forward flux command according to the estimated flux link-age deviation $\Delta\lambda^e{}_{L\,q}$ and $\Delta\lambda^e{}_{L\,d}$ to accelerate the correction of flux linkage during

ISSN No: 2348-4845
International Journal & Magazine of Engineering, Technology, Management and Research
A Peer Reviewed Open Access International Journal

the compensator starting transient. Details of the feed forward command calculator and the design pro-cess are given in [25]. The flux linkage controller eventually produce the voltage command $v_{\lambda}^{e*}{}_{q}$, as shown in Fig. 3. The complete command voltages of the sag compensator are established by the summation of $v_{\lambda}^{e*}{}_{q}$ and v_{xq}^{e*} (from the voltage and current closed-loop control). The proposed control method enables the voltage sag compensator to perform an excellent load voltage tracking and prevent the inrush current in the load transformer.

TABLE I
PARAMETERS OF THE CONTROLLER

K_{pv}	K_{pi}	K_{pt}	$K_{p\lambda}$	$K_{I\lambda}$
1	3.2	400	13	100

In practical application, the load transformer may operate at the saturation knee of the *B–H* curve. Slight flux linkage deviation after the voltage restoration could easily cause a high inrush current. To take this issue into account, the feed forward control design can be integrated into the flux linkage control loop to improve the performance of correction of flux linkage deviation after the sag compensator is activated.

Thus, the impact of the magnetic saturation and the inrush current can be further reduced. Moreover, if the transformer flux linkage can be controlled within the saturation threshold when the voltage compensation is in progress, the flux estimation and the inrush mitigation does not need to consider the saturation characteristic of the magnetizing inductance (L_m).

III. LABORATORY TEST RESULTS

A prototype voltage sag compensator with the proposed in-rush current mitigation technique is implemented in the laboratory. The one-line diagram is as given in Fig. 1. The system parameters of the test bench and the corresponding controller are given as follows (see Table I):

1) source: 220 V, 60 Hz;
2) loads: a commercially available diode rectifier rated at 1600 V with load resistor R = 93.3 Ω, dc choke L = 2.0 mH, and dc filter capacitor C = 3300 μF;
3) voltage sag compensator: a conventional three-phase inverter switching at 10 kHz, the leakage inductance of the coupling transformer L_f = 0.32 mH, and filter capacitor C_f = 4.0 μF;
4) Load transformer: 5.0 kVA, 220 V/127 V (Delta/Wye connection).

Fig. 10 shows the experimental results of the voltage sag compensator without the inrush current mitigation technique under the type D of the phase-to-phase sag in IEEE P1668 standard. The controller detects the voltage sag in 2.0 ms after the fault occurs and injects the required compensation voltage immediately to restore the load voltage, as shown in Fig. 10(b). The transformer flux-linkage dc offsets caused by the voltage sag can be clearly observed in Fig. 10(c), which results in a significant inrush current of peak value 20 A, as shown in Fig. 10(d). Fig. 10(e) shows the transformer flux linkage $\lambda^{e}_{L\,d}$ under the syn-chronous reference frame and the desired flux linkages $\Delta\lambda^{e}_{L\,d}$ ($=\lambda^{e}_{L}{}^{*}_{d} - \lambda^{e}_{L\,d}$) oscillates due to the voltage compensation, and it eventually settles into the steady state due to the core losses of the transformer and the power consumption of the load.

The experimental waveforms of the sag compensator sys-tem with the inrush current mitigation technique enabled under the same type D sag are given in Fig. 11. Fig.11 (a) and (b) shows that the proposed inrush current mitigation technique can achieve fast voltage compensation without causing the flux-linkage dc offset during the transient as compared with Fig. 10(c) and (d). Therefore, the inrush current can be completely avoided, as shown in Fig. 11(d). Furthermore, Fig. 11(a) also shows that the proposed inrush current mitigation technique generates an extra voltage to correct the transient flux linkage when the compensation is initiated, as compared to Fig. 10(b). The magnitude of the extra voltage is determined by the control gains in the flux linkage control loop. Fig. 11(d) illustrates the tracking performance of the proposed inrush current mitigation technique. The PI closed-loop control of the flux linkage results in a smooth transient.

The proposed method is also tested under the voltage sag scenarios of IEEE P1668, and results are given in Fig. 12. The results show that the proposed methods successfully suppress the inrush current under these various scenarios, and the flux linkage estimation of the proposed method is effective in all these situations.

ISSN No: 2348-4845
International Journal & Magazine of Engineering, Technology, Management and Research
A Peer Reviewed Open Access International Journal

IV. DISTURBANCE REJECTION CAPABILITY

The disturbance rejection capability can be characterized by the transfer function between the compensator output voltage and the load current. The proposed inrush current mitigation technique utilizes a flux linkage closed-loop control, and this feature elevates even further the disturbance rejection characteristics of the sag compensator for the fundamental frequency of the load current. The conventional voltage and current-feedback control result in the disturbance rejection characteristics given in (11) and (12), which shows the disturbance rejection capability of the compensator with the voltage and current-feedback control plus the proposed inrush current mitigation technique

$$\left\| \frac{i_{Lq}^{e}(s)}{v_{eq}^{e}(s)} \right\| = \frac{L_f C_f s^3 + K_{pi} C_f s^2 + (K_{pv}+1)s + K_{Iv}}{L_f s^2} \quad (11)$$

$$\left\| \frac{i_{Lq}^{e}(s)}{v_{eq}^{e}(s)} \right\| = \frac{L_f C_f s^4 + K_{pi} C_f s^3 + (K_{pv}+1)s^2 + K_{p\lambda} s + K_{I\lambda}}{L_f s^3}. \quad (12)$$

Three assumptions are made to derive (11) and (12), namely 1) cross-coupling terms in the power circuit has been completely decoupled by the controllers; 2) the flux linkage estimator is approximated as an integrator ($1/s$) during the steady-state operation; and 3) the utility is represented by a stiff voltage source.

Fig. 13 illustrates the Bode diagrams of both transfer functions. To compare the performance of these two systems, the control gain $K_{p\lambda}$ of the proposed inrush current mitigation and the control gain K_{Iv} of the conventional voltage and current-feedback control are set at the same value. The proposed inrush current mitigation technique can effectively raise the disturbance rejection at the fundamental frequency, which corresponds to zero frequency of the Bode diagram under the synchronous reference frame. This feature can be summarized in Table II, as higher $K_{I\lambda}$ gain forces lower load voltage errors under loaded conditions.

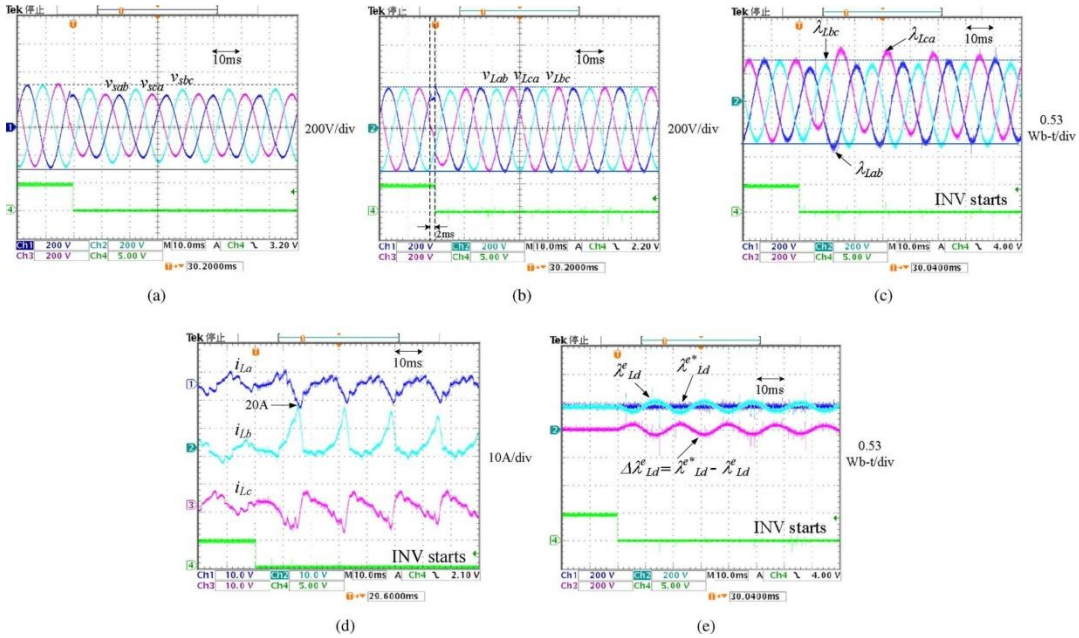

Fig. 10. Test results under a type D voltage sag without the proposed inrush current mitigation technique. (a) Source voltage v_S. (b) Load voltage v_{L-L} (c) Flux linkage of the load transformer λ_{L-L}. (d) Load current i_L. (e) Flux linkage of d-axis $\lambda_{e\,Ld}$.

ISSN No: 2348-4845
International Journal & Magazine of Engineering, Technology, Management and Research
A Peer Reviewed Open Access International Journal

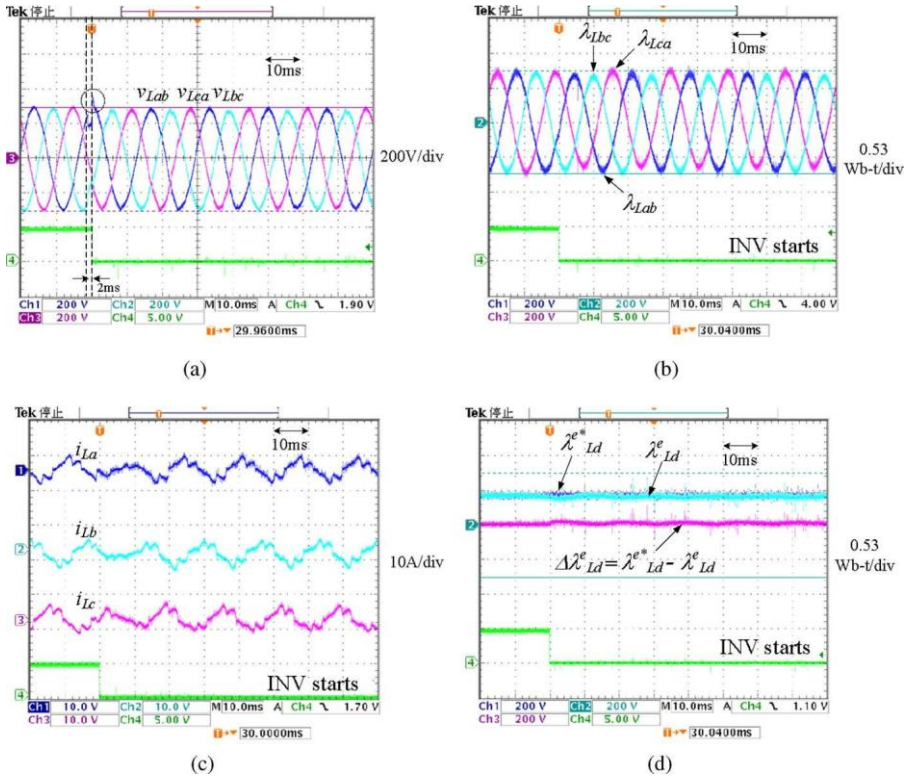

Fig. 11. Test results under a type D voltage sag with the inrush current mitigation technique. (a) Load voltage v_{L-L}. (b) Flux linkage of the load transformer λ_{L-L}. (c) Load current i_L. (d) Flux linkage of d-axis $\lambda_{e\,Ld}$.

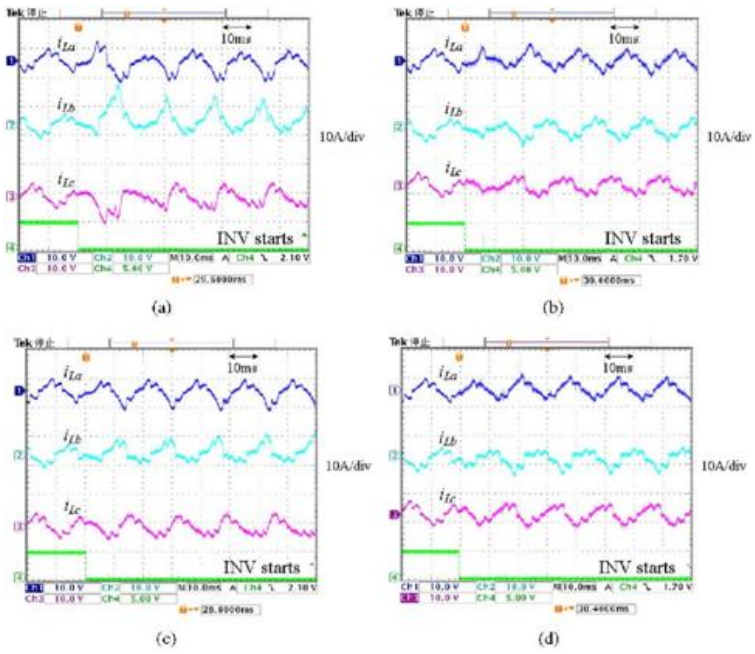

ISSN No: 2348-4845
International Journal & Magazine of Engineering, Technology, Management and Research
A Peer Reviewed Open Access International Journal

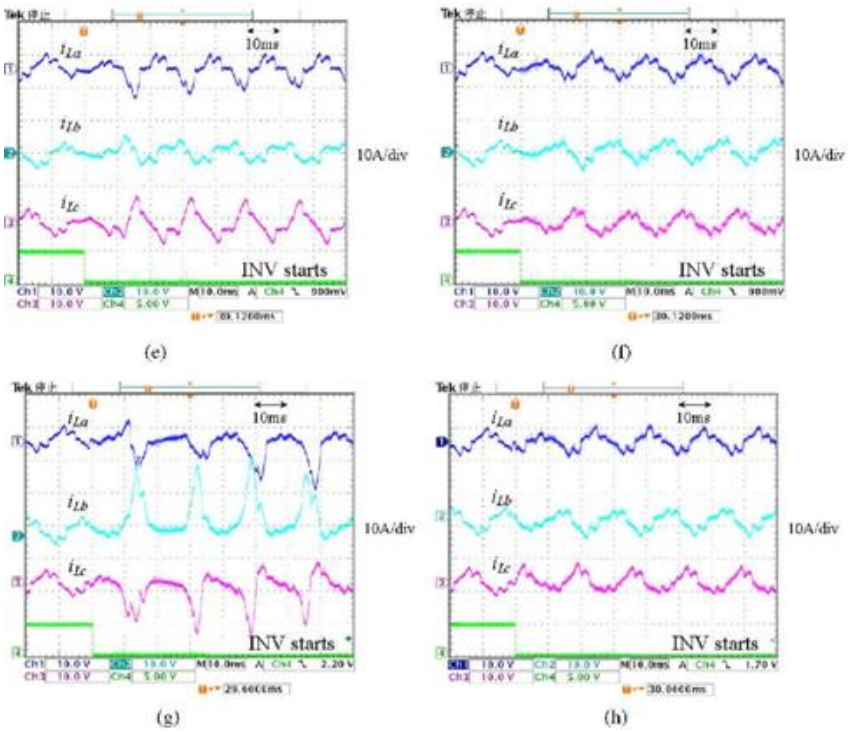

Fig. 12. Load current without and with the inrush current mitigation technique for the sag scenarios of IEEE P1668. (a) Type A sag, without mitigation technique. (b) Type A sag, with mitigation technique. (c) Type B sag, without mitigation technique. (d) Type B sag, with mitigation technique. (e) Type C sag, without mitigation technique. (f) Type C sag, with mitigation technique. (g) Three-phase sags, without mitigation technique. (h) Three-phase sags, with mitigation technique.

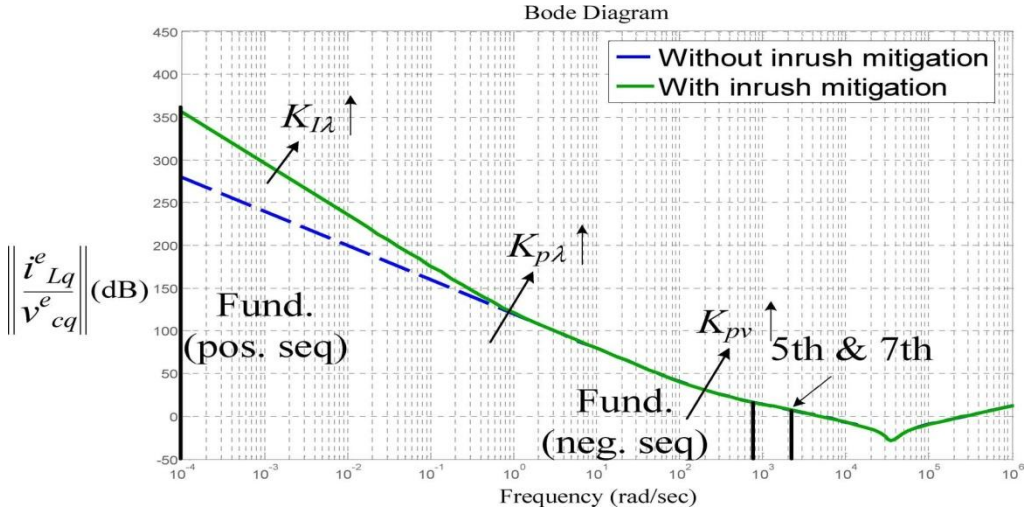

Fig. 13. Comparison between conventional voltage–current state-feedback controller and the proposed inrush current mitigation technique integrated with state-feedback controller in disturbance rejection capability.

ISSN No: 2348-4845
International Journal & Magazine of Engineering, Technology, Management and Research
A Peer Reviewed Open Access International Journal

TABLE II
RELATIONSHIP BETWEEN THE CONTROL GAINS AND THE LOAD VOLTAGE ERRORS

$K_{I\lambda}$ gain	Error of fundamental component of the load voltage
Without inrush current mitigation technique	2.53%
$K_{I\lambda}$=100	1.18%
$K_{I\lambda}$=300	0.91%
$K_{I\lambda}$=1000	0.88%

V. LOAD TRANSFORMER AND COUPLING TRANSFORMER INRUSH MITIGATIONS

One of the advantages of the series-connected sag compensator is that it can restore the load voltage with a converter rated at fractions of the load. A similarly rated coupling transformer is thus adopted for the series connection. As the sag occurs and the compensator engages, both the coupling transformer and the load transformer could face the risk of inrush current. The coupling transformer may have higher potential of magnetic saturation due to its smaller cores. An inrush reduction method for the coupling transformer, proposed by the Cheng *et al.* [24], is illustrated in Fig. 14. As the flux linkage of the coupling transformer reaches a preset level of flux linkage λ_m , the inverter reduces the compensation voltage command v_m^{**} to zero, thus the flux linkage will remain at the present level without the risk of magnetic saturation. The value of λ_m is determined by the saturation knee of the coupling transformer, which can be easily identified.

Fig. 15 shows the integration of the inrush current mitigation controls for both the coupling transformer and the load transformer. The complete voltage command, which combines the

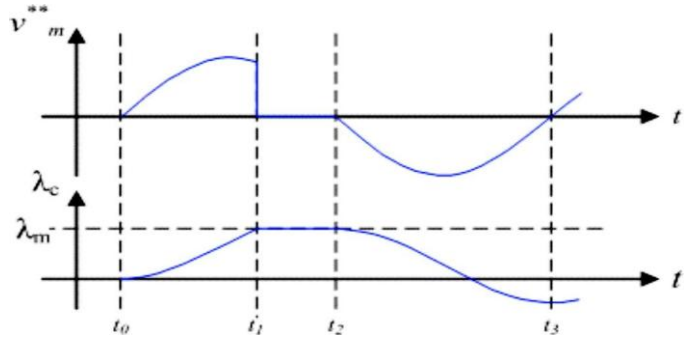

Fig. 14. Simple illustration of the coupling transformer inrush current mitigation proposed in [24].

output of the load transformer flux linkage control ($v_{\lambda q}^{e*}$), and the voltage and current control (v_{xq}^{e*}) is fed into the coupling transformer inrush mitigation control, and its waveform will be modified based on the estimated flux linkage of the coupling transformer, as illustrated in Fig. 14.

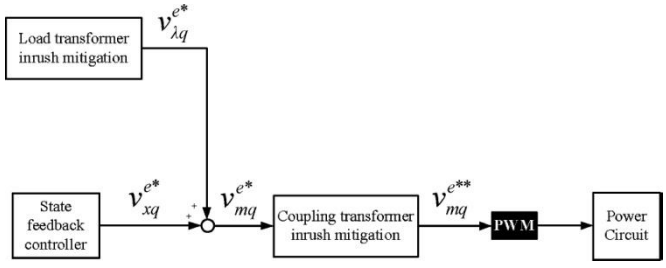

Fig. 15. Integration of the inrush current mitigation of the coupling trans-former and the load transformer.

The load transformer can be successfully avoided as the flux linkage deviation is neutralized once the sag compensator en-gages. The proposed method utilizes the existing voltage and current sensor signals, and thus, it can be easily integrated with the voltage and current control of the sag compensator. Such integration also improves the load disturbance rejection characteristics of the system and stiffens the load voltages against loading variation. The disturbance rejection characteristics of the proposed method

ISSN No: 2348-4845
International Journal & Magazine of Engineering, Technology, Management and Research
A Peer Reviewed Open Access International Journal

are also examined in the frequency do-main for better understanding of the control gains selection and its effect. The effectiveness of the proposed flux linkage compensation method is validated by laboratory test results under various sag scenario of IEEE P1668 standard. The proposed method can also be combined with the inrush reduction method of the coupling transformer presented by the Cheng *et al.* [24], and the test results show that these two methods take effect at different stages of the voltage injection without interfering each other. The integration of these two methods ensures a fast and accurate voltage sag compensation with minimum risk of inrush current.

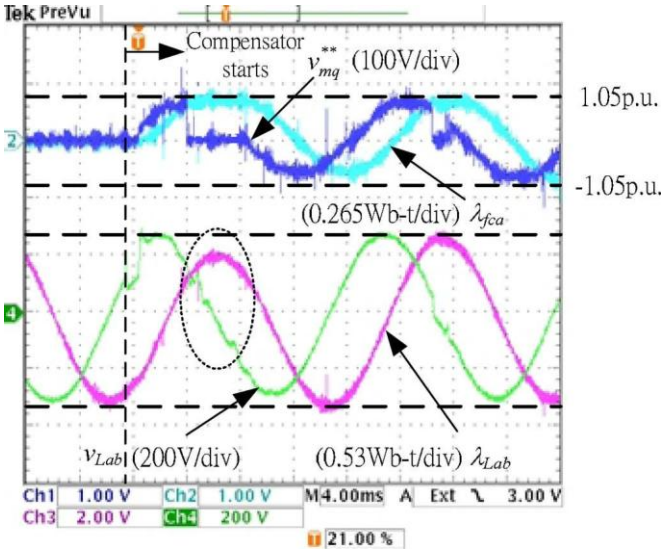

Fig. 16. Coupling transformer flux linkage and compensation voltage (λ_{fca} , $v_{m}^{**}{}_{q}$). Load voltage and load transformer flux linkage (v_{Lab} , λ_{Lab}).

Fig. 16 shows the experimental results of the sag compensator system with both the load transformer inrush mitigation and the coupling transformer inrush mitigation. As the sag compensator starts, the compensation voltage immediately corrects the flux linkage deviation to avoid magnetic saturation of the load trans-former. The compensation voltage command $v_{m}^{**}{}_{q}$ is reduced to zero when the coupling transformer flux linkage reaches the preset limit of 1.05 p.u. to maintain the flux below its saturation knee. Although the flux linkage of the load transformer is af-fected, its closed-loop control will subsequently correct it. These two inrush mitigation methods take effect at different stages of the compensation voltage injection, thus the conflict between the two can be reduced, and both the coupling transformer and the load transformer are relived of the risk of inrush current.

VI. CONCLUSION

An inrush current alleviation system focused around the flux-linkage close-circle control has been proposed for the droop compensator framework in this paper. This synchronous reference-casing based strategy can decisively gauge the flux linkage deviation presented by the disfigured droop voltages inside the heap transformer, and compute the obliged voltage for redressing such deviation progressively. Consequently, the danger of inrush present of the heap transformer can be effectively kept away from as the flux linkage deviation is killed once the hang compensator captivates.

The proposed technique uses the current voltage and current sensor signs, and in this way, it can be effortlessly incorporated with the voltage and current control of the list compensator. Such combination likewise enhances the heap unsettling influence dismissal qualities of the framework and solidifies the heap voltages against stacking variety. The unsettling influence dismissal attributes of the proposed technique are additionally inspected in the recurrence space for better understanding of the control picks up choice and its impact. The viability of the proposed flux linkage recompense technique is approved by research facility test results under different hang situation of IEEE P1668 standard. The proposed system can likewise be joined with the inrush lessening strategy for the coupling transformer exhibited by the Cheng et al. [24], and the test outcomes demonstrate that these two techniques produce results at diverse phases of the voltage infusion without meddling one another. The combination of these two strategies guarantees quick and exact voltage droop remuneration with least danger of inrush current.

ISSN No: 2348-4845
International Journal & Magazine of Engineering, Technology, Management and Research
A Peer Reviewed Open Access International Journal

REFERENCES

[1] D. L. Brooks and D. D. Sabin, "An assessment of distribution system power quality," Elect. Power Res. Inst., Palo Alto, CA, EPRI Final Rep. TR-106249-V2, May 1996, vol. 2.
[2] W. E. Brumsickle, R. S. Schneider, G. A. Luckjiff, D. M. Divan, and M. F. McGranaghan, "Dynamic sag correctors: Cost-effective industrial power line conditioning," *IEEE Trans. Ind. Appl.*, vol. 37, no. 1, pp. 212– 217, Jan./Feb. 2001.
[3] N. H. Woodley, "Field experience with dynamic voltage restorer (DVR^{TM}MV) systems," in *Proc. IEEE Power Eng. Soc. Winter Meeting*, Jan. 23–27, 2000, vol. 4, pp. 2864–2871.
[4] R. Affolter and B. Connell, "Experience with a dynamic voltage restorer for a critical manufacturing facility," in *Proc. IEEE Transmiss. Distrib. Conf. Expo.*, 2003, vol. 3, pp. 937–939.
[5] C. N.-M. Ho, H. S. H. Chung, and K. T. K. Au, "Design and implemen-tation of a fast dynamic control scheme for capacitor-supported dynamic voltage restorers," *IEEE Trans. Power Electron.*, vol. 23, no. 1, pp. 237– 251, Jan. 2008.
[6] C. Meyer, R. W. De Doncker, Y. W. Li, and F. Blaabjerg, "Optimized control strategy for a medium-voltage DVR—Theoretical investigations and experimental results," *IEEE Trans. Power Electron.*, vol. 23, no. 6, pp. 2746–2754, Nov. 2008.
[7] J. G. Nielsen and F. Blaabjerg, "A detailed comparison of system topolo-gies for dynamic voltage restorers," *IEEE Trans. Ind. Appl.*, vol. 41, no. 5, pp. 1272–1280, Sep./Oct. 2005.
[8] M. S. J. Asghar, "Elimination of inrush current of transformers and dis-tribution lines," in *Proc. IEEE Power Electron., Drives Energy Syst. Ind. Growth*, 1996, vol. 2, pp. 976–980.
[9] Y. Cui, S. G. Abdulsalam, S. Chen, and W. Xu, "A sequential phase energization technique for transformer inrush current reduction—Part I: Simulation and experimental results," *IEEE Trans. Power Del.*, vol. 20, no. 2, pp. 943–949, Apr. 2005.
[10] W. Xu, S. G. Abdulsalam, Y. Cui, and X. Liu, "A sequential phase en-ergization technique for transformer inrush current reduction—Part II: Theoretical analysis and design guide," *IEEE Trans. Power Del.*, vol. 20, no. 2, pp. 950–957, Apr. 2005.
[11] P. C. Y. Ling and A. Basak, "Investigation of magnetizing inrush current in a single-phase transformer," *IEEE Trans. Magn.*, vol. 24, no. 6, pp. 3217– 3222, Nov. 1988.
[12] C. Fitzer, A. Arulampalam, M. Barnes, and R. Zurowski, "Mitigation of saturation in dynamic voltage restorer connection transformers," *IEEE Trans. Power Electron.*, vol. 17, no. 6, pp. 1058–1066, Nov. 2002.
[14] G. Zenginobuz, I. Cadirci, M. Erims, and C. Barlak, "Perfor-mance optimization of induction motors during voltage-controlled soft starting," *IEEE Trans. Energy Convers.*, vol. 19, no. 2, pp. 278–288, Jun. 2004.
[15] J. Nevelsteen and H. Aragon, "Starting of large motors-methods and eco-nomics," *IEEE Trans. Ind. Appl.*, vol. 25, no. 6, pp. 1012–1018, Nov./Dec. 1989.
[16] H. Yamada, E. Hiraki, and T. Tanaka, "A novel method of suppressing the inrush current of transformers using a series-connected voltage-source PWM converter," in *Proc. IEEE Power Electron. Drives Syst. PEDS 2005 Int. Conf.*, 2006, vol. 1, pp. 280–285.
[17] S. Martinez, M. Castro, R. Antoranz, and F. Aldana, "Off-line uninter-ruptible power supply with zero transfer time using integrated magnetics," *IEEE Trans. Ind. Electron.*, vol. 36, no. 3, pp. 441–445, Aug. 1989.
[18] C.-C. Yeh and M. D. Manjrekar, "A reconfigurable uninterruptible power supply system for multiple power quality applications," *IEEE Trans. Power Electron.*, vol. 22, no. 4, pp. 1361–1372, Jul. 2007.
[19] *IEEE Recommended Practice for the Design of Reliable Industrial and Commercial Power Systems*, IEEE Standard 493-2007, 2007.
[20] P. T. Cheng, J. M. Chen, and C. L. Ni, "Design of a state-feedback con-troller for series voltage sag compensators," *IEEE Trans. Ind. Appl.*, vol. 45, no. 1, pp. 260–267, Jan./Feb. 2009.
[21] J. G. Nielsen, M. Newman, H. Nielsen, and F. Blaabjerg, "Control and testing of a dynamic voltage restorer (DVR) at medium voltage level," *IEEE Trans. Power Electron.*, vol. 19, no. 3, pp. 806–813, May 2004.
[22] M. Vilathgamuwa, A. A. D. R. Perera, and S. S. Choi, "Performance im-provement of the dynamic voltage restorer with closed-loop load voltage and current-mode control," *IEEE Trans. Power Electron.*, vol. 17, no. 5, pp. 824–834, Sep. 2002.
[23] M. J. Ryan, W. E. Brumsickle, and R. D. Lorenz, "Control topology options for single-phase UPS inverters," *IEEE Trans. Ind. Appl.*, vol. 33, no. 2, pp. 493–501, Mar./Apr. 1997.
[24] *Recommended Practice for Voltage Sag and Interruption Ride-Through Testing for End-Use Electrical Equipment Less Than 1,000 Volts*, IEEE IAS P1668 Voltage Sag Ride-through Working Group, Dec. 2004.
[25] P. T. Cheng, W. T. Chen, Y. H. Chen, C. L. Ni, and J. Lin, "A transformer inrush mitigation method for series Voltage sag compensators," *IEEE Trans. Power Electron.*, vol. 22, no. 5, pp. 1890–1899, Sep. 2007.
[26] Y. H. Chen, "Voltage sag ride-through solutions based on solid-state trans-fer switches and uninterruptible power supplie," Ph.D. dissertation, Dept. Electr. Eng., National Tsing Hua Univ., to be published in July 2010.

ISSN No: 2348-4845
International Journal & Magazine of Engineering, Technology, Management and Research
A Peer Reviewed Open Access International Journal

ABOUT AUTHORS

P.SUDHEER, PG student, Department of Electrical & Electronics Engineering, P.V.K.K Institute of Technology, JNTU Anantapuramu, Andhra Pradesh, INDIA.
Email: sudher.0224@gmail.com

B.HARI PRASAD, Assistant Professor, Department of Electrical & Electronics Engineering, P.V.K.K Institute of Technology JNTU Anantapuramu, Andhra Pradesh, INDIA.
Email: vanoorhari@gmail.com

G.N.S.VAIBHAV, M.TECH (EPS), Head Of the Department, PVKK Institute of Technology, JNTU Anantapuramu, Andhra Pradesh, INDIA.
Email: vaibhavnaidu.naidu@gmail.com